

Synthesis and Characterization of Palladium(II) and Nickel(II) Alcoholate-Functionalized NHC Complexes and of Mixed Nickel(II)–Lithium(I) Complexes

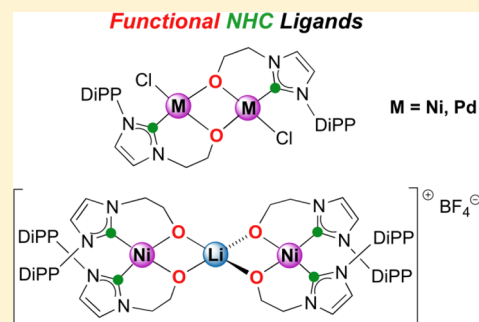
Sophie Hameury,[†] Pierre de Frémont,[†] Pierre-Alain R. Breuil,[‡] Hélène Olivier-Bourbigou,[‡] and Pierre Braunstein^{*,†}

[†]Laboratoire de Chimie de Coordination, Institut de Chimie (UMR 7177 CNRS), Université de Strasbourg, 4 rue Blaise Pascal, CS 90032, 67081 Strasbourg, France

[‡]IFP Energies nouvelles, Rond-Point de l'Echangeur de Solaize, 69360 Solaize, France

Supporting Information

ABSTRACT: The synthesis of Pd(II) and Ni(II) alcohol-functionalized N-heterocyclic carbene (NHC) complexes was explored to examine the possible influence of the functional arm attached to the NHC backbone on their structure and reactivity and, in the case of a Ni(II) complex, on its catalytic properties in ethylene oligomerization. Starting from the alcohol-functionalized imidazolium salt [ImDiPP(C₂OH)]Cl (**2**), the new functionalized NHC palladium(II) complex [PdCl(acac){ImDiPP(C₂OH)-C_{NHC}}] (**3**) was synthesized and fully characterized. Two byproducts, [PdCl{μ-ImDiPP(C₂O)-C_{NHC}O}]₂ (**4**) and *trans*-[PdCl₂{ImDiPP(C₂OH)-C_{NHC}}]₂ (**5**), formed during the synthesis of **3**, were also fully characterized. Acids promoted the transformation of **3** into the new C_{NHC}-bound complex [PdCl(μ-Cl){ImDiPP(C₂OH)-C_{NHC}}]₂ (**6**), unveiling the lability of the acac ligand and the resistance of the Pd–NHC bond to acids. Complex **6** reacted with a base to afford complex **4**, in which alkoxide coordination to Pd(II) has occurred to generate a C_{NHC}O chelate. The stability of **3** was also assessed under basic conditions, and the new complex [Pd(acac){ImDiPP(C₂O)-C_{NHC}O}] (**7**) was characterized. The new nickel(II) alcoholate-functionalized NHC complex [NiCl{μ-ImDiPP(C₂O)-C_{NHC}O}]₂ (**8**) was synthesized by the reaction of the imidazolium salt **2** with *n*-BuLi and [NiCl₂(dme)]. The reaction of **8** with HCl regenerates the imidazolium and alcohol functions to give [ImDiPP(C₂OH)]₂[NiCl₄] (**9**). The mixed-metal Ni(II)–Li(I) complexes [Ni₂{μ-ImDiPP(C₂O)-C_{NHC},μ-O}]₄LiBF₄ (**10**), [Ni₂{μ-ImDiPP(C₂O)-C_{NHC},μ-O}]₄LiCl (**11**), and [Ni{ImDiPP(C₂O)-C_{NHC},μ-O}]₂LiBr (**12**) were isolated and characterized. However, it was not possible to synthesize a Ni(II) alcohol-functionalized NHC complex in high yield. Small amounts of the square-planar complex [NiCl₂{ImDiPP(C₂OH)-C_{NHC}}]₂ (**13**) could be isolated, and this complex was characterized by single-crystal X-ray diffraction. In **13**, only the C_{NHC} atom of the alcohol-functionalized NHC ligand is bound to the metal. The structures of the imidazolium salt 2·2H₂O and of the complexes **3**, **4**, **4-polymorph**, **5**, **6**·CH₂Cl₂, and **8**–**13** were established by single-crystal X-ray diffraction.



INTRODUCTION

There has been a recent emphasis on hybrid ligands containing at least one N-heterocyclic carbene (NHC) donor group (for recent reviews, see e.g. ref 1). Depending on the donor strength of the functional group associated with the NHC moiety, a NHC metal complex with a dangling functionality or with a stabilizing, spectator chelating hybrid ligand may result. The formation of a chelate reduces the tendency of the ligand to dissociate and, because of the chemically different nature of the donor groups, it brings about stereoelectronic differentiation within the metal coordination sphere.^{1c,2} Furthermore, a hemilabile metal–ligand system may result that could display increased catalytic activity in comparison to a static chelate.^{1c,3} In nickel(II) chemistry, numerous heterobidentate NHCs have been synthesized and coordinated through both donor functions, which include not only neutral groups, such as heterocycles,⁴ phosphines,^{4b,5} amines,⁶ amides,⁷ or imines⁸ but

also anionic donors, the latter being increasingly studied because of their stronger interaction with the metal center.^{1b,f} The objectives of the present work are 2-fold: (i) examine the coordination behavior of alcohol/alcoholate-functionalized NHC ligands with Pd(II) and Ni(II) and expand the number of still rare Ni(II) complexes containing potentially bidentate NHC-alcohol/alcoholate ligands and (ii) evaluate the properties of the resulting Ni(II) complexes in catalytic ethylene oligomerization. Palladium(II) complexes bearing oxygen-functionalized NHC ligands appear more widespread and involve ether,⁹ alcohol,^{9,10} alcoholate,¹⁰ enolate,¹¹ phenol,¹² and phenolate functions.^{12,13} Recent reviews have highlighted the catalytic properties of Pd–NHC complexes in carbon–carbon coupling reactions.¹⁴ In 2012, Pd(II) complexes bearing a

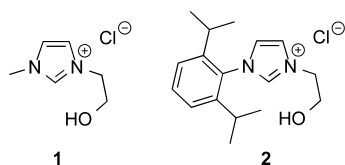
Received: February 12, 2014

Published: April 25, 2014

pyridine-functionalized NHC ligand were found to be active in ethylene oligomerization, which illustrates the importance of hybrid ligands containing at least one NHC moiety in catalysis.¹⁵ Whereas Pd(II)–NHC complexes are usually easily characterized because of their diamagnetic nature and lower reactivity, Ni(II)–NHC chemistry remains challenging and can provide paramagnetic mixtures that are difficult to analyze. We are aware that the coordination of the alcohol function to give a C_{NHC}OH chelating ligand may be difficult to achieve. However, coordination of an alcoholate donor to Ni(II) should be easier and worth exploring, since deprotonation of both the alcohol and the imidazolium moieties of the proligand could lead to an analogue of the anionic P,O-type ligands involved in SHOP-type ethylene oligomerization catalysts.¹⁶ Until 2013, only a few nickel(II) complexes containing an NHC donor linked to an oxygen-functionalized arm such as imidates,¹⁷ enolates,¹⁸ and phenolates¹⁹ were reported. Mixed NHC-alcoholate ligands have appeared more recently,^{10f,20} and the first two alcoholate-functionalized NHC nickel complexes were reported in 2013.²¹ The first complex was a chiral NHC ligand comprising a binaphthyl moiety further coordinated to nickel and formed an active catalyst in norbornene polymerization.^{21a} The second example was based on a fluoroalkoxy carbene which led to a mixture of two complexes: one was bis-chelated by the hybrid ligand, and the other was monochelated and retained a phosphine ligand from the precursor complex.^{21b} Catalytic ethylene oligomerization directed toward the synthesis of short-chain α -olefins remains a topic of considerable academic and industrial interest, and it is well established that minor changes in the ligand properties may be sufficient to significantly influence the activity and selectivity of nickel catalysts.^{16,22} We wish to examine here how an oxygen functionality attached to an NHC moiety could influence the catalytic properties of their nickel(II) complexes for this reaction.

RESULTS AND DISCUSSION

Palladium Complexes. We first examined the reactivity of the proligands **1** and **2** toward palladium(II), which should produce tetracoordinate, diamagnetic square-planar complexes, readily amenable to characterization by NMR spectroscopy. In order to have access to alcohol-functionalized NHC complexes, we used the methodology developed by Nolan et al. to attempt the synthesis of [PdCl(acac)(NHC)] complexes without affecting the alcohol moiety.²³ Our first attempts to synthesize such complexes were performed using [ImMe(C₂OH)]Cl (**1**; 3-(2-hydroxyethyl)-1-methyl-1*H*-imidazol-3-ium chloride) as ligand precursor, but owing to a lack of solubility of the imidazolium salt and of the products formed, we were not able to isolate any pure complex. In order to improve the solubility of the compounds, the size of the N substituent was increased and [ImDiPP(C₂OH)]Cl (**2**; 1-(2,6-diisopropylphenyl)-3-(2-hydroxyethyl)-1*H*-imidazol-3-ium chloride) was used instead.



Single crystals of $2 \cdot 2\text{H}_2\text{O}$ were analyzed by X-ray diffraction (Figure 1). The imidazolium salt **2** crystallizes in the monoclinic system with the $P2_1/c$ space group. In the unit

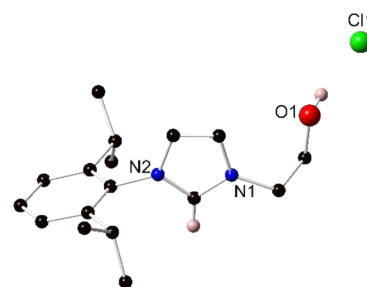


Figure 1. Ball and stick representation of [ImDiPP(C₂OH)]Cl (**2**) in $2 \cdot 2\text{H}_2\text{O}$. Hydrogen atoms have been omitted for clarity, except for the OH and azolium protons. An ORTEP drawing with 30% probability ellipsoids is provided in Figure S1 of the Supporting Information.

cell, the chloride anions interact with the hydroxyl groups by hydrogen bonding; they also interact with the NCHN protons. The asymmetric unit contains three imidazolium chloride entities and two molecules of water. The N1–C1 and N2–C1 bond lengths are 1.329(3) and 1.336(3) Å, respectively, and the N1–C1–N2 angle ($108.4(2)^\circ$) is similar to that in other imidazolium salts.²⁴

Proligand **2** was refluxed in dioxane with [Pd(acac)₂] for 2 days.²³ ¹H NMR spectroscopy supported the deprotonation of the imidazolium function and revealed the formation of a major product, **3**, and at least two minor products, **4** and **5** that were difficult to separate (Scheme 1). Unlike its application to nonfunctionalized NHCs,²³ this strategy is thus not straightforward in our case and was slightly modified (see below).

The ¹H NMR spectrum of the major product **3**, similarly to the case of the nonfunctionalized NHC Pd–acac complexes, reveals an inhibition of the free rotation of the carbene ligand.²⁵ Consequently, the signals attributed to the alcohol chain and to the CH^{ipr} and CH₃^{ipr} protons from the DiPP group are broad in CD₂Cl₂. The aromatic signals of the DiPP groups of the ligand are almost unaffected in comparison to the proligand **2**. The CH protons of the imidazole backbone are shifted upfield by 0.82 and 0.22 ppm, and the OH signal is strongly shifted upfield (2.8 ppm). The CH^{ipr} and the CH₂ protons of the alcohol functions are shifted downfield by 0.29, 0.14, and 0.27 ppm, respectively. The signals at 5.31, 1.91, and 1.87 ppm, which account respectively for the CH^{acac-Pd} and CH₃^{acac-Pd} protons, are different from those in [Pd(acac)₂] and confirm the formation of the anticipated [PdCl(acac)(NHC)] complex. The signals sharpen in DMSO, and the inequivalence of the four CH₃^{ipr} groups confirms again the hindered rotation about the Pd–C bond. The ¹³C NMR spectrum of **3** displays a signal at 150.0 ppm, attributed to the Pd-bound carbene; this value is in the range of those reported for other [PdCl(acac)(NHC)] complexes.^{23b,25} The mass spectrum of the complex displays a major peak corresponding to [Pd(acac)(NHC–OH)]⁺.

The structure of **3** was determined by X-ray diffraction on single crystals obtained by slow diffusion of pentane into a saturated CH₂Cl₂ solution, which established its nature as [PdCl(acac){ImDiPP(C₂OH)-C_{NHC}}] (**3**) (Figure 2).

Complex **3** crystallizes in the orthorhombic system with the *Pbca* space group. The Pd(II) center displays a square-planar geometry, being surrounded by ligand **2** acting as a C_{NHC} donor (Pd–C = 1.954(4) Å), a terminal chloride (Pd–Cl = 2.2768(10) Å), and a chelating acac group. The angles around the Pd(II) center are 88.11(12), 92.56(11), 90.17(10), and 89.18(8)^o for C1–Pd–O1, O1–Pd–O2, C1–Pd–Cl1, and O2–Pd–Cl1, respectively. The Pd–O bond in a position trans

Scheme 1. Synthesis of Complexes 3–5

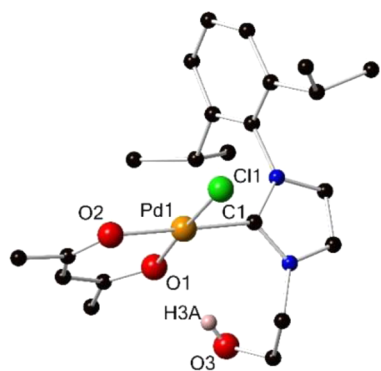
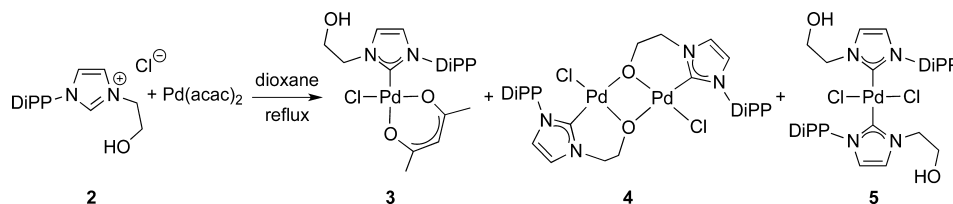


Figure 2. Ball and stick representation of $[\text{PdCl}(\text{acac})\{\text{ImDiPP}-(\text{C}_2\text{OH})-\text{C}_{\text{NHC}}\}]$ (3). Hydrogen atoms have been omitted for clarity, except for the OH proton. An ORTEP drawing with 30% probability ellipsoids is provided in Figure S2 of the Supporting Information.

to the carbene ligand (2.041(3) Å) is longer than that trans to the chloride (2.013(2) Å), owing to the stronger trans influence of the NHC ligand in comparison to Cl^- . All bond lengths are in agreement with the literature values for comparable bonds.²⁵ Interestingly, an intramolecular hydrogen-bonding interaction is observed between the alcohol proton and an oxygen of the acac moiety.

The formation of 3 was accompanied by that of two byproducts, which were readily isolated because of their rapid crystallization (in comparison to that of 3) from a CH_2Cl_2 /pentane or ether solution. Thus, orange and yellow crystals of $[\text{PdCl}\{\mu\text{-ImDiPP}(\text{C}_2\text{O})-\text{C}_{\text{NHC},\text{O}}\}]_2$ (4) and *trans*- $[\text{PdCl}_2\{\text{ImDiPP}(\text{C}_2\text{OH})-\text{C}_{\text{NHC}}\}_2]$ (5), respectively, were obtained (Figures 3 and 4).

Complex 4 crystallizes in the monoclinic system with the $P2_1/c$ space group with two possible unit cell parameters (Supporting Information). It is worth noting that there is no solvent molecule in the unit cell, making both crystalline forms

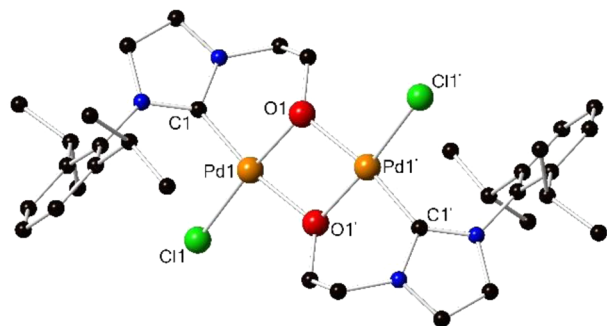


Figure 3. Ball and stick representation of $[\text{PdCl}\{\mu\text{-ImDiPP}(\text{C}_2\text{O})-\text{C}_{\text{NHC},\text{O}}\}]_2$ (4). Hydrogen atoms have been omitted for clarity. An ORTEP drawing with 30% probability ellipsoids is provided in Figure S3 of the Supporting Information.

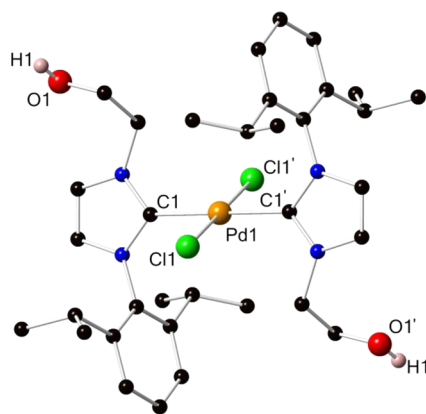


Figure 4. Ball and stick representation of *trans*- $[\text{PdCl}_2\{\text{ImDiPP}-(\text{C}_2\text{OH})-\text{C}_{\text{NHC}}\}_2]$ (5). Hydrogen atoms have been omitted for clarity, except for the OH protons. An ORTEP drawing with 30% probability ellipsoids is provided in Figure S4 of the Supporting Information.

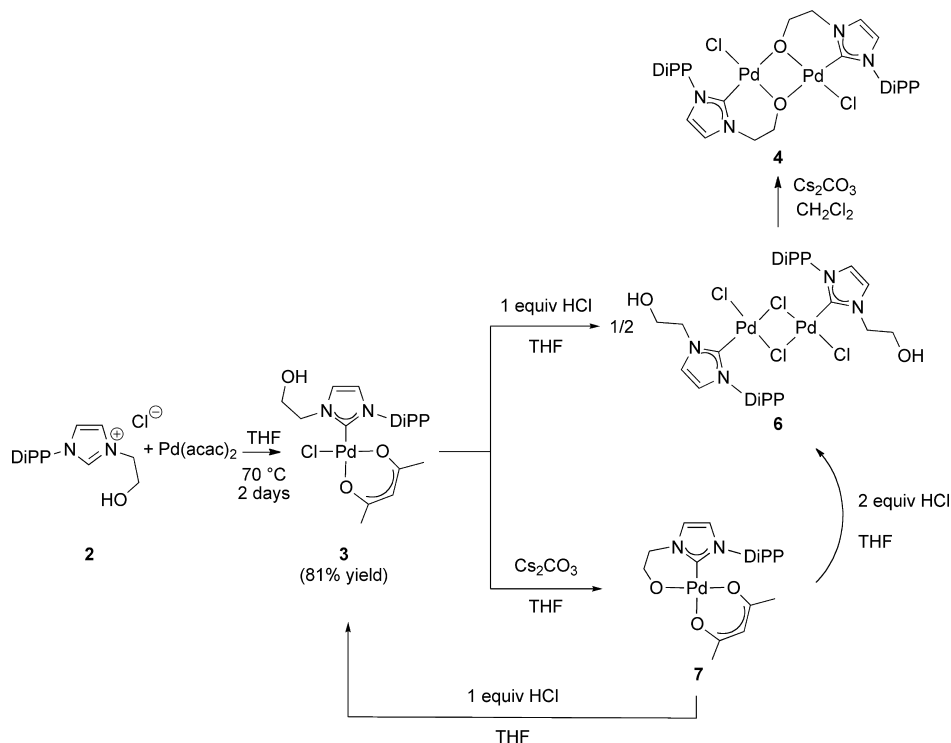
true polymorphs easily distinguishable by their different colors (pale yellow 4 vs deep orange 4-polymorph). The main structural difference concerns the presence (or absence) of positional disorder affecting the oxygen atoms bridging the palladium centers. The structure of 4 exhibits a dinuclear complex with two equivalent Pd(II) centers, $\text{C}_{\text{NHC}}\text{O}$ chelated by the ligands and bridged by the alcoholate groups (the $\text{Pd1}-\text{O}-\text{Pd1}'$ angle is $100.67(8)^\circ$). The square-planar coordination sphere of each Pd(II) center is completed by a terminal chloride. The interligand angles are $90.00(9)$, $79.33(8)$, $95.47(8)$, and $95.20(5)^\circ$ for $\text{C1}-\text{Pd}-\text{O1}$, $\text{O1}-\text{Pd}-\text{O1}'$, $\text{C1}-\text{Pd}-\text{Cl1}$, and $\text{O1}'-\text{Pd}-\text{Cl1}$, respectively. The length of the Pd–O bond trans to the carbene is larger than that trans to the chloride ligand (2.075(2) and 2.025(2) Å), consistent with the stronger trans influence of the NHC donor. The Pd– $\text{C}_{\text{carbene}}$ and Pd–Cl bond lengths of 1.940(3) and 2.2893(7) Å, respectively, are similar to those for 3.

To the best of our knowledge, only five examples of dinuclear Pd–NHC complexes comprising two $\mu\text{-O}$ bridges have been reported: two with alkoxides²⁶ and three with hydroxides as bridges.²⁷ The metrical data of 4 are in excellent agreement with those reported for these complexes. We will see below that the alcoholate-functionalized NHC Pd(II) complex 4 could be accessed in a more rational manner.

Complex 5 crystallizes in the monoclinic system with the $P2_1/c$ space group, and the palladium atom is situated on a center of symmetry for the molecule (Figure 4).

Two *trans* NHC moieties are C_{NHC} -coordinated to the Pd(II) center, and the coordination sphere of the metal is completed with two terminal chlorides, providing a square-planar environment with interligand angles of $90.64(9)$, $89.36(9)$, $89.36(9)$, and $90.634(9)^\circ$ for $\text{C1}-\text{Pd}-\text{Cl1}'$, $\text{C1}'-\text{Pd}-\text{Cl1}'$, $\text{C1}-\text{Pd}-\text{Cl1}$, and $\text{C1}'-\text{Pd}-\text{Cl1}$, respectively. The Pd–C and Pd–Cl bond lengths of 2.030(3) and 2.3179(8) Å,

Scheme 2. Formation of the Pd(II) Complex 3 from 2 and Its Reactivity under Basic or Acidic Conditions (See Text)



respectively, are in the range of those reported for other $[\text{PdCl}_2(\text{NHC})_2]$ complexes.²⁸ Intermolecular hydrogen bonding occurs between the alcohol proton and the chloride ligands, resulting in a 1-D polymeric arrangement (see Figure S12 in the Supporting Information).

The methodology used to prepare 3 was then modified in order to prevent the formation of 4 and 5. THF was used as a solvent, and the reaction temperature was decreased to 70°C , thus leading to a longer (2 days) but cleaner reaction (Scheme 2).

Performing the reaction at lower temperature was unsuccessful, since the conversion stopped at 55% after 5 days, even though fewer impurities were formed. Complex 3 is moisture- and air-stable but decomposed slowly during chromatography through silica, with formation of a new complex observable by NMR spectroscopy but not characterized. Purification was performed by rapid filtration through a thin plug of silica, using ethyl acetate as solvent, and was followed by precipitation from CH_2Cl_2 /pentane and washings with pentane to remove the traces of acetylacetonate formed, giving 3 as a yellow powder in 81% yield.

The stability of 3 toward acidic conditions was tested using 1 equiv of HCl (Scheme 2). The formation of a new complex was confirmed by ^1H NMR analysis, the disappearance of the signals due to the acac moiety indicating its protonation/decoordination. The signals of the alcohol chain and of the CH^{iPr} and CH_3^{iPr} protons remained broad, as for 3, indicating hindered rotation of the carbene ligand. The CH protons of the imidazole backbone were shifted downfield by 0.30 and 0.25 ppm in comparison to those for 3. The signals of the DiPP groups were almost unaffected by the decoordination of the acac ligand, with no significant shift for the $\text{CH}^{\text{m-Ar}}$ and CH_3^{iPr} protons. The CH^{iPr} signal was shifted slightly upfield. The protons of the CH_2 group were shifted in the opposite direction. In the ^{13}C NMR spectrum, the carbenic signal

appeared at 142.8 ppm. The acac ligand was likely replaced by a chloride arising from the HCl used. Note that, similarly to 3, the ^1H NMR signals became sharper in polar solvent such as CD_3CN , and no coordination of the nitrile was observed.

These hypotheses were confirmed by the structure determination of $[\text{PdCl}(\mu\text{-Cl})\{\text{ImDiPP}(\text{C}_2\text{OH})\text{-C}_{\text{NHC}}\}]_2$ (6) by X-ray diffraction on single crystals obtained by slow diffusion of pentane into a saturated solution of CH_2Cl_2 (Figure 5).

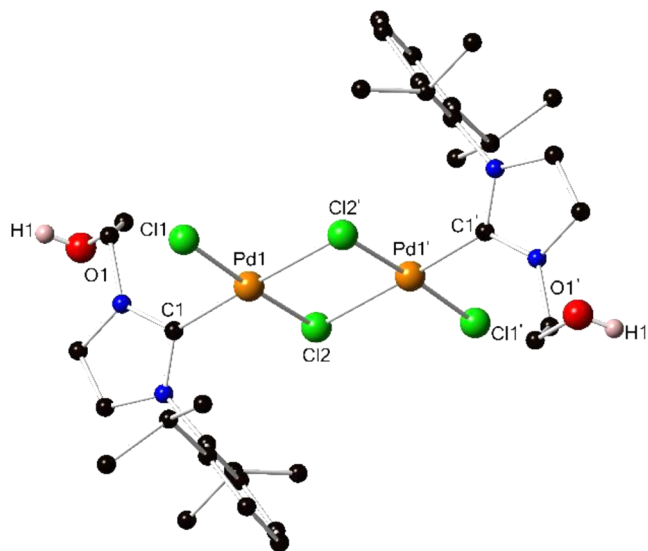


Figure 5. Ball and stick representation of $[\text{PdCl}(\mu\text{-Cl})\{\text{ImDiPP}(\text{C}_2\text{OH})\text{-C}_{\text{NHC}}\}]_2$ (6) in $6\cdot\text{CH}_2\text{Cl}_2$. Hydrogen atoms have been omitted for clarity, except for the OH protons. An ORTEP drawing with 30% probability ellipsoids is provided in Figure S5 of the Supporting Information.

Complex **6** cocrystallizes with CH_2Cl_2 molecules in the monoclinic system with the $P2_1/c$ space group. The centrosymmetric structure of **6** contains two Pd(II) centers coordinated by the monodentate C-bound NHC ligand, a terminal chloride, and two bridging chlorides. The square-planar coordination geometry around the metals is characterized by typical angles of 89.6(2), 92.0(2), 91.98(7), and 86.40(7)° for C1–Pd1–Cl1 or C1'–Pd1–Cl1', C1–Pd1–Cl2 or C1'–Pd1–Cl2', Cl1–Pd1–Cl2' or Cl1'–Pd1–Cl2, and Cl2–Pd1–Cl2' or Cl2–Pd1'–Cl2', respectively. The Pd1–(μ -Cl2)–Pd1' angle is 93.60(7)°. The Pd–C_{carbene} and Pd–Cl_{terminal} bond lengths are 1.975(5) and 2.290(2) Å. The Pd–Cl_{bridging} distance trans to the carbene is longer than that trans to the terminal chloride (2.412(2) and 2.315 (2) Å), consistent with the stronger trans influence of the NHC donor. These values are in the range of those reported for other $[\text{Pd}_2(\mu\text{-Cl})_2\text{X}_2(\text{NHC})_2]$ complexes.²⁹ H bonding is present between the alcohol groups and the terminal chlorides.

Quite surprisingly, we did not observe decomposition of **6** in the presence of excess hydrochloric acid by carbon–palladium bond cleavage and imidazolylidene reprotonation, which emphasizes the resistance of the Pd^{II}–C_{carbene} bond. The complex **6** was isolated in 84% yield as a yellow powder. Its mass spectrum displayed a major peak at m/z 687.25, which could not be assigned, and another signal corresponded to $[\text{Pd}_2\text{Cl}_3\{\text{ImDiPP}(\text{C}_2\text{OH})\}_2]^+$.

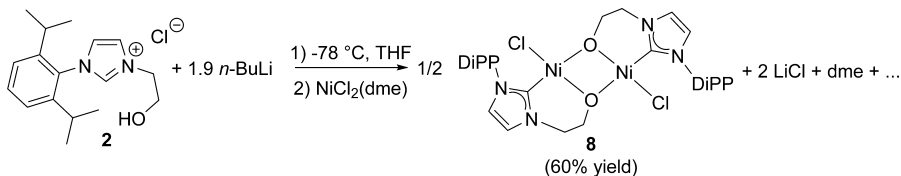
Complex **6** was then reacted with Cs_2CO_3 in order to form an alcoholate that could subsequently coordinate to palladium (Scheme 2). Gratifyingly, this strategy was successful, as evidenced by NMR spectroscopy, since a sharpening of the broad signals characteristic of **3** and **6** was observed in CD_2Cl_2 . Furthermore, no alcohol proton was visible. In comparison to **6**, the signals were respectively shifted upfield by 0.15 and 0.16 ppm for the $\text{CH}^{m\text{-Ar}}$ and $\text{CH}^{p\text{-Ar}}$ protons, 0.21 and 0.27 ppm for the imidazole backbone, and 0.88 and 1.17 ppm for the CH_2 and CH_2O groups. The latter two shifts highlight the coordination of the alcoholate function. Furthermore, this coordination gave rise to diastereotopic protons at the CH_2 and CH_2O groups, even though overlap of the signals provided two multiplets.³⁰ The signals accounting for the CH_3^{iPr} and CH^{iPr} groups were the only ones shifted downfield (0.09 and 0.28 ppm for CH_3^{iPr} and 0.06 ppm for CH^{iPr}). In the ^{13}C NMR spectrum, the carbenic signal appeared at 147.0 ppm. Crystals suitable for X-ray diffraction analysis were grown by stratification of a CH_2Cl_2 solution of **4** with pentane. A preliminary cell measurement indicated the formation of **4**, which was one of the byproducts observed during the formation of **3**. The ^{13}C NMR value for the carbene signal of complex **4** was in the range of those reported for other $[\text{Pd}_2\text{X}_2(\mu\text{-O})_2(\text{NHC})_2]$ complexes.^{27c} The mass spectrum of **4** displayed a major peak at m/z 832.16 which could not be assigned, although its isotopic distribution supported the retention of a dinuclear palladium structure in the gas phase. A second signal was also observed at m/z 791.13 corresponding to $[\text{Pd}_2\text{Cl}(\text{ImDiPP}(\text{C}_2\text{O}))_2]^+$.

Reaction of **4** with a slight default of HCl did not lead to the clean re-formation of **6**. Although the ^1H NMR spectrum of the crude reaction mixture indicated that **6** is the major reaction product, at least two other new complexes formed, which were not further characterized. Surprisingly, a peak at 8.62 ppm appeared, possibly indicating partial reprotonation of the NHC ligand.

The stability of **3** toward a basic medium was also assessed, using Cs_2CO_3 (Scheme 2). Two products were observed in the crude reaction mixture in a 9:1 ratio, by ^1H NMR spectroscopy, when the reaction was performed in CH_2Cl_2 . The major product, **7**, is a new palladium complex, while the minor product is **4**. Both products were separated by fractional crystallization using CH_2Cl_2 /pentane. Formation of **4** could be prevented by addition of a large excess of base in the presence of 1 equiv of acetylacetone to avoid its decoordination. Similarly to **4**, coordination of the alcoholate moiety led to a sharpening of the ^1H NMR signals in comparison to **3** in CD_2Cl_2 . All of the signals were shifted upfield, by 0.17 and 0.20 ppm for the $\text{CH}^{m\text{-Ar}}$ and $\text{CH}^{p\text{-Ar}}$ groups, by 0.23 and 0.28 ppm for the imidazole backbone, and by 0.77 and 0.74 ppm for the CH_2 and CH_2O groups, respectively. Similarly to **4**, the large displacement of the CH_2 and CH_2O signals revealed the coordination of the alkoxide chain to palladium and their multiplicity confirmed the diastereotopicity of these protons. The signals accounting for the CH_3^{iPr} and CH^{iPr} groups were the only ones shifted downfield (0.03 and 0.11 ppm for CH_3^{iPr} and 0.19 ppm for CH^{iPr}). The signals of the acac moiety resonated at 5.03 ppm for CH^{acac} and at 1.84 and 1.00 ppm for the $\text{CH}_3^{\text{acac}}$, which indicated retention of its coordination to palladium. Thus, the expected formula for this new complex is $[\text{Pd}(\text{acac})\{\text{ImDiPP}(\text{C}_2\text{O})\text{-C}_{\text{NHC}}\text{O}\}]$ (**7**). The ^{13}C NMR spectrum revealed a carbenic signal at 151.6 ppm, a value which is in the range of those reported for other $[\text{PdCl}(\text{acac})\text{-}(\text{NHC})]$ complexes.^{23,25} Surprisingly, the presence of an interacting molecule of water was indicated by a ^1H NMR signal at 1.65 ppm instead of 1.52 ppm; it could not be removed even after prolonged heating under vacuum. The results of the elemental analyses confirmed the formulation $[\text{Pd}(\text{acac})\{\text{ImDiPP}(\text{C}_2\text{O})\text{-C}_{\text{NHC}}\text{O}\}]\cdot\text{H}_2\text{O}$ for $7\cdot\text{H}_2\text{O}$, in agreement with the ^1H NMR data. The mass spectrum of complex **7** displayed a major peak corresponding to $[\text{Pd}(\text{acac})\{\text{ImDiPP}(\text{C}_2\text{OH})\}]^+$, which indicated reprotonation of the alkoxide during analysis. Despite numerous attempts, no crystals suitable for X-ray diffraction analysis could be obtained.

The reaction of complex **7** with 1 equiv of HCl led to the re-formation of **3** by clean reprotonation of the alcoholate moiety (Scheme 2). Further addition of HCl led to the formation of **6** (Scheme 2). It is worth mentioning that all of the palladium complexes were air- and moisture-stable.

Nickel Complexes. Initial attempts to prepare a nickel(II) carbene complex from **1** or **2** proved difficult. Similarly to what was described above for Pd(II), attempts to synthesize a Ni–NHC complex starting from the imidazolium salt **1** were unsuccessful, due to the lack of solubility of the ligand and of the product(s) formed. The use of a nickel precursor containing an internal base, similarly to the methodology used with palladium, was revealed to be ineffective. Several bases and metallic precursors with adjusted stoichiometry were used to perform either the single or double deprotonation of the alcohol/azolium functions. Activation of the C–H bond of the imidazolium salt with a Ni(0) precursor was also attempted. Despite several attempts, none of these reagents proved to be efficient (NaH , Cs_2CO_3 , $\text{Ni}(\text{CO})_3$, $\text{Ni}(\text{OAc})_2$, $[\text{Ni-Me}_2(\text{tmeda})]$, or $[\text{Ni}(\text{cod})_2]$). In all cases, we could only detect the precursors or a mixture of decomposition products, which could not be separated or characterized. We have recently reported different attempts to apply the silver transmetalation route to the synthesis of alcohol-functionalized NHC Ni(II) complexes, but only reprotonation of the C2

Scheme 3. Optimized Reaction Conditions for the Synthesis of $[\text{NiCl}\{\mu\text{-ImDiPP}(\text{C}_2\text{O})\text{-C}_{\text{NHC}}\text{O}\}]_2$ (**8**)

carbon of the carbene ligand was observed.³¹ Despite our efforts, no alcohol-functionalized NHC Ni(II) complex could be synthesized in a rational manner. Therefore, the synthesis of an alcoholate-functionalized NHC ligand was attempted.

We attempted to isolate and characterize the free carbene ligand, or its alkali-metal adduct, starting from **2**. Double deprotonation of tertiary alcohol–NHC proligands with a lithiated base, *n*-BuLi or LiHMDS (lithium hexamethyldisilazide), has been known since 2004 to afford Li–alcoholate/Li–NHC adducts with pseudocubane structures.³² Unfortunately, we could not characterize any product because, after deprotonation, the ¹H NMR signals remained very broad, even at low or high temperature, and X-ray-quality crystals could not be grown. However, a one-pot synthetic approach involving direct reaction of the deprotonated mixture with a nickel(II) salt appeared to be a promising alternative to the unsuccessful transmetalation route. It would not require the isolation of fully characterized free or alkali-metal-adduct NHC species prior to metalation.

Following this approach, the double deprotonation of **2** was performed with *n*-BuLi, followed by the direct addition of $[\text{NiCl}_2(\text{dme})]$. The complex $[\text{NiCl}\{\mu\text{-ImDiPP}(\text{C}_2\text{O})\text{-C}_{\text{NHC}}\text{O}\}]_2$ (**8**) was obtained, with some byproducts (at least one of them being paramagnetic) (Scheme 3).

A screening of various reaction conditions was performed. Replacing *n*-BuLi with KHMDS (potassium hexamethyldisilazide) did not improve the yield but rather resulted in the enhanced formation of paramagnetic byproducts. We also tried different reaction times, temperatures, and solvents, such as toluene, diethyl ether, and THF, but could not decrease the quantity of byproducts formed. The best results were obtained when *n*-BuLi was added at $-78\text{ }^\circ\text{C}$ to a THF solution of **2**, and after the reaction mixture was stirred for 3 h, solid $[\text{NiCl}_2(\text{dme})]$ was added and the reaction mixture was slowly warmed to room temperature overnight. The stoichiometry of the base was then optimized for these reaction conditions, and using a slight default of *n*-BuLi (1.9 equiv) was found beneficial, since any excess base resulted in an increased formation of byproducts (Scheme 3). Upon precipitation from THF, complex **8** and LiCl could be separated from the impurities that remained soluble in THF. Then, **8** was dissolved in CH_2Cl_2 , the solution was filtered through Celite to remove LiCl, and **8** was reprecipitated by addition of Et_2O , affording a purple powder in 60% yield. The formation of diamagnetic **8** was confirmed by ¹H NMR spectroscopy. The disappearance of the signals for the NCHN and OH acidic protons was observed. The imidazole protons gave rise to two doublets with ³*J*(H–H) = 1.7 Hz, instead of two doublets of doublets (³*J*(H–H) and ⁴*J*(H–H)) in **2**, consistent with the deprotonation of the imidazolium moiety and resulting disappearance of the ⁴*J*(H–H) coupling. In comparison to those of the imidazolium salt **2**, both imidazole signals were shifted upfield by 1.29 and 0.55 ppm and the $\text{CH}^{\text{p-Ar}}$ and the $\text{CH}^{\text{m-Ar}}$ signals were shifted upfield by 0.15 and 0.08 ppm, respectively. Both CH^{iPr} signals

and one of the CH_3^{iPr} signals were shifted downfield by 0.54 and 0.83 ppm, respectively, whereas the other CH_3^{iPr} signal did not show any significant shift drift (0.03 ppm). The chemical shifts of the CH_2 and the CH_2O protons were highly sensitive to the coordination of the alcoholate to nickel, since both signals were shifted upfield by 0.79 and 1.74 ppm, respectively. We could not observe the carbene signal by ¹³C NMR, directly or indirectly (HMBC correlation experiment). Complex **8** decomposed slightly during the NMR experiments, forming an intractable paramagnetic product in nondry NMR solvent. The use of dry solvents under an inert atmosphere slowed the decomposition of **8** without completely stopping it. Complex **8** displayed a pronounced instability in solution (THF , CH_2Cl_2 , Et_2O), and the decomposition products could not be analyzed, owing to their paramagnetic and amorphous nature. The mass spectrum of **8** displayed two intense peaks, one for $[(\text{NHC})\text{-H}]^+$ and the other, unassigned, having an isotopic distribution indicating the presence of two ligands for one metal center. Furthermore, the molecular peak corresponding to $[\text{Ni}_2\text{Cl}(\text{NHC})_2]^+$ was visible, with a very weak intensity. Considering the large amount of reprotonated ligand visible in the mass spectrum, it is reasonable to assume that **8** is unstable under the analysis conditions.

Purple X-ray-quality crystals of **8** were grown by slow diffusion of pentane into a CH_2Cl_2 solution of the complex (Figure 6).

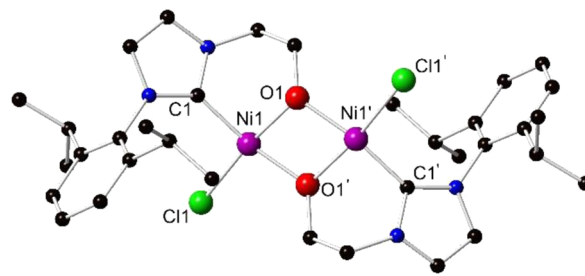


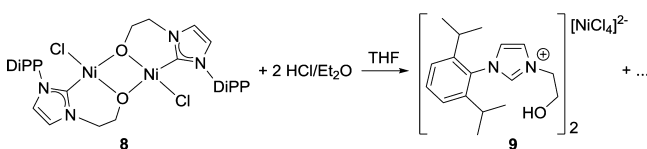
Figure 6. Ball and stick representation of $[\text{NiCl}\{\mu\text{-ImDiPP}(\text{C}_2\text{O})\text{-C}_{\text{NHC}}\text{O}\}]_2$ (**8**). Hydrogen atoms have been omitted for clarity. An ORTEP drawing with 30% probability ellipsoids is provided in Figure S6 of the Supporting Information.

Complex **8** crystallizes in the monoclinic system with the $P2_1/c$ space group. Its molecular structure is depicted in Figure 6. In this centrosymmetric dinuclear complex, similarly to the palladium complex **4**, each nickel(II) center is C,O-chelated. The Ni centers have a distorted-square-planar coordination geometry, with the angles around the metal of $92.30(14)$, $77.74(12)$, $94.71(12)$, and $95.43(8)^\circ$ for O1-Ni1-C1 , O1-Ni1-O1' , C1-Ni1-Cl1 , and O1'-Ni1-Cl1 , respectively. The alcoholate functions form bridges between the two metal centers with a Ni1-O1-Ni1' angle of $102.26(12)^\circ$. The metal coordination sphere is completed by a terminal chloride. The $\text{Ni-C}_{\text{carbene}}$ bond length is $1.876(4)\text{ \AA}$, and the Ni-O distance

trans to the carbene is longer than that trans to the chloride ligand (1.914(3) vs 1.868(3) Å), in agreement with the stronger trans influence of the NHC donor. A recently reported thiolato-bridged dinuclear Ni^{II}-NHC complex with metal centers in a square-planar coordination environment presents a similar structure.³³ However, this complex was synthesized under harsher conditions, unlike ours, by reacting the thioester-functionalized imidazolium salt with [Ni(OAc)₂] in molten [N(*n*-Bu)₄]Br under vacuum at 120 °C for 16 h.

The stability of **8** was also assessed in the presence of an acid (Scheme 4). In contrast to the Pd(II) chemistry shown above,

Scheme 4. Formation of [ImDiPP(C₂OH)]₂[NiCl₄] (9**) from **8** in the Presence of HCl**



the complex is not stable under acidic conditions, since addition of HCl in diethyl ether to a THF solution of **8** led to the formation of a paramagnetic blue solution. Deep blue crystals suitable for X-ray diffraction were grown directly from the THF reaction mixture, and their analysis revealed the formation of [ImDiPP(C₂OH)]₂[NiCl₄] (**9**) (Figure 7), in contrast with

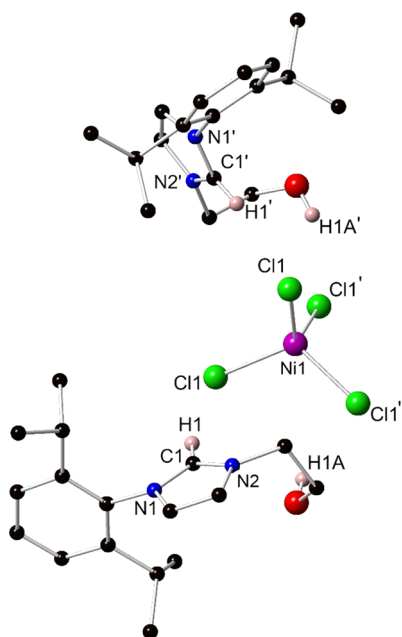


Figure 7. Ball and stick representation of [ImDiPP(C₂OH)]₂[NiCl₄] (**9**). Hydrogen atoms have been omitted for clarity, except for the azolium and OH protons. An ORTEP drawing with 30% probability ellipsoids is provided in Figure S7 of the Supporting Information.

other situations, where the Ni^{II}-NHC bond was stable toward HCl addition.³⁴ Reprotonation of the carbene and alcoholate moieties likely represent possible decomposition pathways for **8** in solution (Scheme 4).

Compound **9** crystallizes in the tetragonal system with the $I\bar{4}$ space group. In the unit cell, the [NiCl₄]²⁻ anions display the expected tetrahedral coordination geometry and are positioned on the 4-fold symmetry axes. The chlorides of [NiCl₄]²⁻

interact with the hydroxyl groups by hydrogen bonding. In the imidazolium moiety, the N1–C1 and N2–C1 bond lengths are 1.333(3) and 1.325(3) Å, respectively, and the N1–C1–N2 angle is 108.3(2)°. The metrical data are similar to those observed in **2** (see above).

After optimization of the synthesis of **8** using a ligand/metal/base ratio of 1/1/1.9, we explored the ratio 2/1/2, hoping that similar reaction conditions could be applied. The base used in combination with ligand **2** was *n*-BuLi in THF, and different metallic precursors were tested, [Ni(NCMe)₄](BF₄)₂, [NiCl₂(dme)], and [NiBr₂(dme)] (Scheme 5). Although we had to face reproducibility and sensitivity issues, we were able in each case to isolate crystals of one of the products formed, but only in small quantities.

When [Ni(NCMe)₄](BF₄)₂ was used as the precursor in the reaction with **2** (Scheme 5), a yellow solution was obtained. During ¹H NMR monitoring of different reactions, we observed two different situations: either partial deprotonation of the ligand and coordination to nickel (some of the imidazolium salt was not deprotonated) or complete disappearance of the NCHN proton and formation of a mixture of complexes (full deprotonation of the salt). Note that NMR spectra of the reaction mixture are reported in the Supporting Information with the assignment of some characteristic signals. Although we were not able to separate all the products formed, we could crystallize one of them in small quantities by slow diffusion of hexane in a THF solution and its formulation and structure, [Ni₂{μ-ImDiPP(C₂O)-C_{NHC}μ-O}₄Li]BF₄ (**10**), were established by X-ray diffraction analysis (Figure 8).

The bimetallic Ni–Li complex **10** crystallizes in the monoclinic system with the P₂₁/c space group. Two molecules of THF are present in the unit cell and were omitted due to high thermal displacements (squeeze procedure during the refinement). Each nickel(II) center is C,O-bis-chelated and features a square-planar coordination geometry with tetrahedral distortion (the interligand angles around nickel are in the range 96.55(11)–85.97(8)°). The Ni–C_{carbene} bond lengths are slightly shorter than those found in **8**. The alcoholate functions bridge between the Ni(II) and Li(I) centers with angles in the range 95.58(15)–96.27(15)°. The lithium cation is bis-chelated by a neutral Ni(II) metalloligand, and the four alcoholate donors generate a distorted, flattened tetrahedral coordination geometry for the Ni(II) center, with Ni–O–Li angles ranging from 81.8(2) to 134.7(3)°. The electroneutrality of the complex is ensured by an external BF₄⁻.

During one of our attempts to reproduce the synthesis of **10**, we isolated from the crude reaction mixture colorless crystals suitable for X-ray diffraction and their analysis as 2·2H₂O revealed the re-formation of the imidazolium salt (see Figure 1).

When the complex [NiCl₂(dme)] was used as the precursor (Scheme 5), the ¹H NMR spectrum of the crude reaction mixture indicated complete deprotonation of the imidazolium salt by the disappearance of the NCHN acidic proton signal. Furthermore, no trace of the alcohol proton was found. However, the formation of a mixture of two different complexes in a 1/1 ratio was observed. The NMR spectra of the reaction mixture are reported in the Supporting Information, with the assignment of some characteristic signals. Unfortunately, we were not able to separate these products by the usual techniques (fractional crystallization, extraction, precipitations, ...). The products were air- and moisture-sensitive and decomposed on silica, ruling out any possible separation by

Scheme 5. Bimetallic Ni–Li Complexes 10–12 Obtained (Low Yields) from Different Ni Precursor Complexes

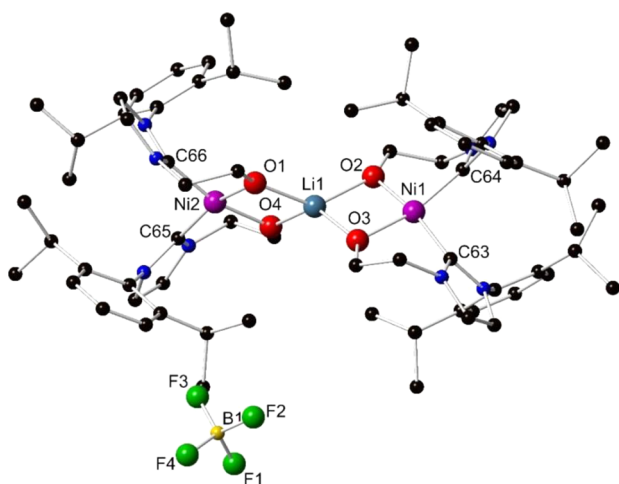
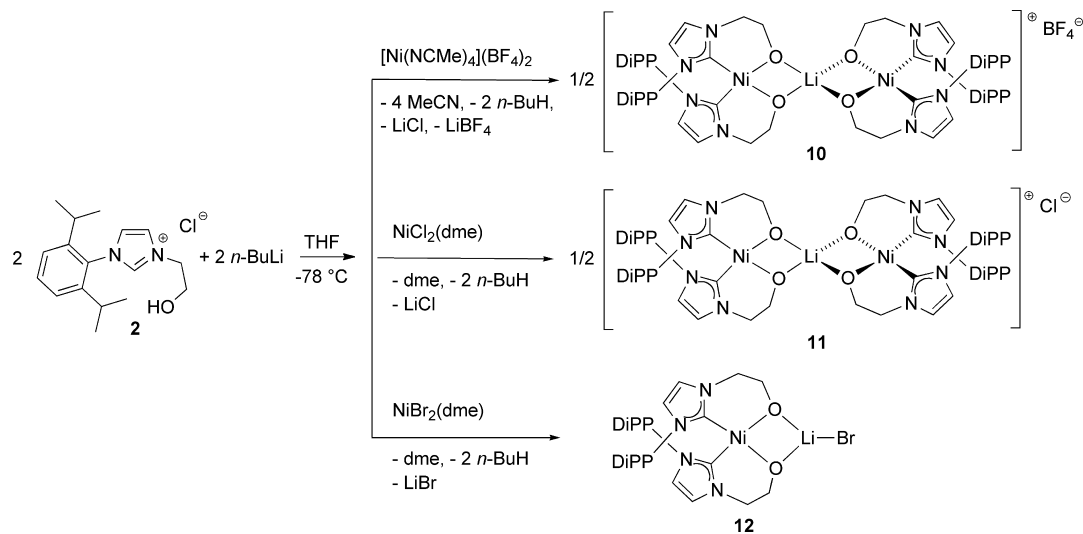


Figure 8. Ball and stick representation of $[\text{Ni}_2\{\mu\text{-ImDiPP}(\text{C}_2\text{O})\text{-C}_{\text{NHC}}\mu\text{-O}\}_4\text{Li}]\text{BF}_4$ (**10**). Hydrogen atoms have been omitted for clarity. An ORTEP drawing with 30% probability ellipsoids is provided in Figure S8 of the Supporting Information. Selected bond distances (Å) and angles (deg): Ni–C63 1.836(3), Ni–C64 1.831(2), Ni–C65 1.835(3), Ni–C66 1.842(2), Ni–O1 1.876(2), Ni–O2 1.882(2), Ni–O3 1.883(2), Ni–O4 1.887(2); C64–Ni1–C63 96.55(11), C64–Ni1–O2 91.10(9), C63–Ni1–O3 90.77(10), O2–Ni1–O3 85.93(8), C65–Ni2–C66 97.76(11), C66–Ni2–O1 90.20(9), C65–Ni2–O4 90.33(9), O1–Ni2–O4 85.97(8), Ni2–O1–Li 96.27(15), Ni1–O2–Li 95.67(15), Ni1–O3–Li 95.58(15), Ni2–O4–Li 95.91(15), O2–Li–O1 134.7(3), O2–Li–O3 82.8(2), O3–Li–O4 133.4(3), O4–Li–O1 81.8(2).

column chromatography. Instead of directly reacting 2 equiv of free NHC generated *in situ* with $[\text{NiCl}_2(\text{dme})]$, another route was attempted to synthesize selectively only one of the possible products, and complex **8** was reacted with 2 equiv of deprotonated **2**, thus retaining the 2/1 ligand/metal ratio. The same ^1H NMR spectra were obtained, and after several crystallizations were attempted to separate the products, we isolated, on one occasion only, yellow crystals of the complex $[\text{Ni}_2\{\mu\text{-ImDiPP}(\text{C}_2\text{O})\text{-C}_{\text{NHC}}\mu\text{-O}\}_4\text{Li}]\text{Cl}$ (**11**) in a small amount by stratification of a THF solution with diethyl ether used as cosolvent. The molecular structure of the Ni–Li complex **11** is very similar to that of **10**, except that the

electroneutrality of the complex is ensured by external Cl^- instead of BF_4^- . All of the structural details and bonding parameters are provided in the Supporting Information (Figure 9).

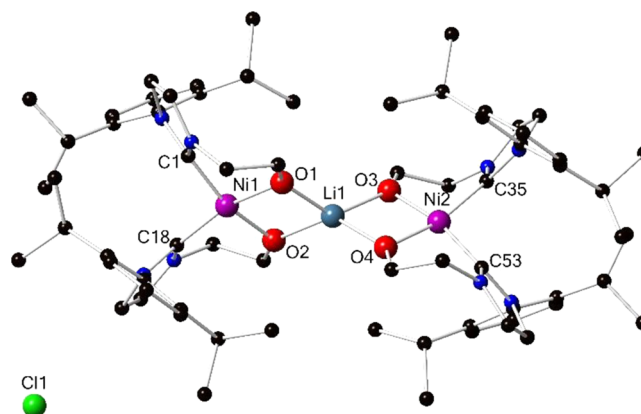


Figure 9. Ball and stick representation of $[\text{Ni}_2\{\mu\text{-ImDiPP}(\text{C}_2\text{O})\text{-C}_{\text{NHC}}\mu\text{-O}\}_4\text{Li}]\text{Cl}$ (**11**). Hydrogen atoms have been omitted for clarity. An ORTEP drawing with 30% probability ellipsoids is provided in Figure S9 of the Supporting Information. Selected bond distances (Å) and angles (deg): Ni–C1 1.851(3), Ni–C18 1.836(3), Ni–C35 1.835(3), Ni–C53 1.837(3), Ni–O1 1.887(2), Ni–O2 1.881(2), Ni–O3 1.891(3), Ni–O4 1.883(2); C18–Ni1–C1 98.55(14), C18–Ni1–O2 90.29(11), C1–Ni1–O1 89.82(12), O2–Ni1–O1 85.77(9), C53–Ni2–C35 97.08(14), C53–Ni2–O4 90.72(12), C35–Ni2–O3 90.49(13), O4–Ni2–O3 85.79(10), O1–Li1–O2 82.0(2), O1–Li1–O3 132.5(3), O2–Li1–O4 134.7(3), O3–Li1–O4 82.2(2).

The bimetallic (Ni/Li) complex **11** crystallizes in the monoclinic system with the $P2_1/c$ space group. There are some cocrystallized molecules of solvent located around the special positions in the unit cell, but they could not be modeled properly from the difference electron density map (squeeze procedure during the refinement). The Ni–C_{carbene} bond lengths are between 1.835(3) and 1.851(3) Å. The nickel center displays a distorted-square-planar coordination geometry, and the lithium is in a distorted-tetrahedral environment, similarly to what was observed for **10**. All bond lengths and angles are very similar to those in **10**.

Finally, when $[\text{NiBr}_2(\text{dme})]$ was used as precursor (Scheme 5), the ^1H NMR spectrum of the crude reaction mixture indicated again that **2** was not completely deprotonated and we were not able to obtain a pure complex in a significant amount. The ^1H NMR spectrum of the reaction mixture is reported in the Supporting Information, with the assignment of some characteristic signals. Yellow crystals suitable for X-ray diffraction analysis were obtained by slow evaporation of a benzene solution of the crude reaction mixture. The structure of $[\text{Ni}\{\text{ImDiPP}(\text{C}_2\text{O})\text{-C}_{\text{NHC}}\mu\text{-O}\}_2\text{LiBr}]$ (**12**) is depicted in Figure 10.

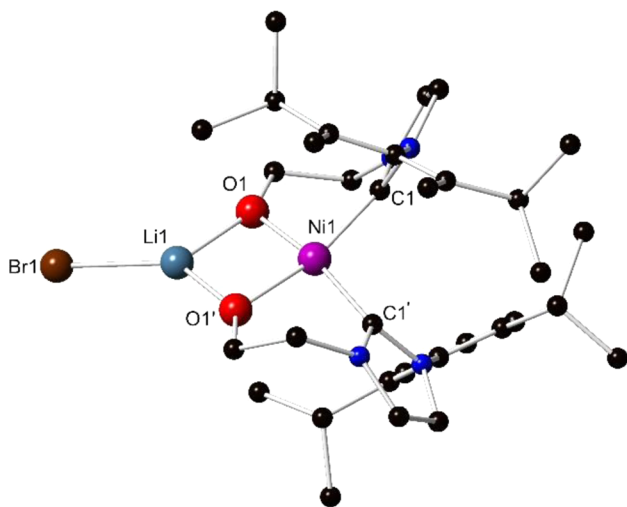


Figure 10. Ball and stick representation of $[\text{Ni}\{\text{ImDiPP}(\text{C}_2\text{O})\text{-C}_{\text{NHC}}\mu\text{-O}\}_2\text{LiBr}]$ (**12**). Hydrogen atoms have been omitted for clarity. An ORTEP drawing with 30% probability ellipsoids is provided in Figure S10 of the Supporting Information.

The bimetallic Ni–Li complex **12** crystallizes in the monoclinic system with the $C2/c$ space group. The nickel(II) center is C,O-bis-chelated by the functional NHC ligand and features a distorted-square-planar coordination geometry, with angles of $97.5(2)$, $90.5(1)$, $90.5(1)$, and $85.6(1)^\circ$ for C1–Ni–C1', C1'–Ni–O1', C1–Ni–O1, and O1–Ni–O1', respectively. A 2-fold symmetry axis for the molecule passes through the Li and Ni atoms. The Ni–C_{carbene} and Ni–O bond lengths are 1.833(3) and 1.892(2) Å, respectively. The alcoholate functions bridge between the Ni(II) and Li(I) centers, with a Li–O1–Ni angle of $93.0(2)^\circ$. The Li cation is chelated by the Ni(C_{NHC}O)₂ moiety acting as a metalloligand, and its coordination sphere is completed by a terminal bromide. This provides the lithium cation with a trigonal coordination geometry, less common than the tetrahedral coordination found in **10** and **11**, with angles of $88.5(4)$, $135.7(2)$, and $135.8(2)^\circ$ for O1–Li–O1', O1–Li–Br, and O1'–Li–Br, respectively.³⁵

In the course of various attempts to reproduce the synthesis of **11**, the mononuclear complex $[\text{NiCl}_2\{\text{ImDiPP}(\text{C}_2\text{OH})\text{-C}_{\text{NHC}}\}_2]$ (**13**) was isolated, in a very small amount, as orange crystals suitable for X-ray diffraction analysis (Figure 11). This complex likely results from the reprotonation of the alcoholate groups bound to nickel in complex **11**. After redissolution of these crystals in CD_2Cl_2 , a ^1H NMR spectrum was recorded, but the signals were too broad to be assigned. A singlet resonance at 9.99 ppm is assigned to an azolium function

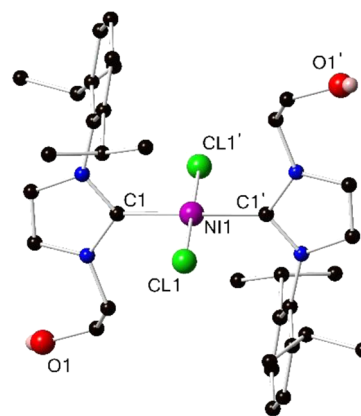


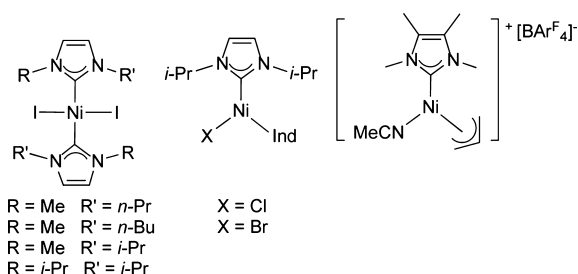
Figure 11. Ball and stick representation of $[\text{NiCl}_2\{\text{ImDiPP}(\text{C}_2\text{OH})\text{-C}_{\text{NHC}}\}_2]$ (**13**). Hydrogen atoms have been omitted for clarity, except for the OH protons. An ORTEP drawing with 30% probability ellipsoids is provided in Figure S11 of the Supporting Information.

resulting from the decoordination/reprotonation of the Ni-bound imidazolylidene donors in complex **13**.

Complex **13** crystallizes in the monoclinic system with the $P2_1/c$ space group. The Ni atom occupies a center of symmetry for the molecule and is coordinated by two trans C_{NHC} donors and two chlorides, forming a square-planar coordination environment with angles of $90.97(8)$, $89.03(8)$, $89.03(8)$, and $90.97(8)^\circ$ for C1–Ni–Cl1', C1'–Ni–Cl1', C1–Ni–Cl1, and C1'–Ni–Cl1, respectively. The Ni–C and Ni–Cl bond lengths are 1.918(3) and 2.1922(7) Å, respectively. Similarly to its Pd(II) analogue **5**, intermolecular interactions between the alcohol groups and the chlorides result in the formation of a polymeric chain but there is no inter- or intramolecular interaction between the alcohol groups and the nickel center (see Figure S13 in the Supporting Information). The metrical data of **13** are in excellent agreement with those reported for similar square-planar bis-NHC Ni(II) dichloride complexes.^{8,31,36}

Catalytic Ethylene Oligomerization. Simple Ni(II)–NHC complexes have been tested as precatalysts in ethylene oligo- and polymerization but were revealed to be poorly active because of the reductive elimination of the ligand that can occur during catalysis.³⁷ The introduction on the NHC ligand of a functional arm that may coordinate to the metal center in the precatalysts or in the active species may prevent such deactivation reactions by conferring additional stability through the chelate effect and by enforcing a rigid conformation unsuitable for reductive elimination.^{1c,2} The catalytic activity of **8** for ethylene oligomerization was examined in combination with 10 equiv of ethylaluminum dichloride (EADC) as cocatalyst using chlorobenzene as solvent (see details in the Supporting Information). An activity of 11100 (g of C₂H₄)/(g of Ni) (TON = 23100 (mol of C₂H₄)/(mol of Ni)) was obtained after 35 min, which corresponds to a productivity of 19000 (g of C₂H₄)/((g of Ni) h) and a TOF value of 39800 (mol of C₂H₄)/((mol of Ni) h). The selectivities for C₄ olefins and 1-butene were 56 and 6 mol %, respectively. Interestingly, a related phenoxy-functionalized NHC ligand was found to act as a C_{NHC}–O chelate toward Ni(II), but the resulting complex was inactive toward ethylene.^{19c,38} An indenyl Ni(II) complex with a non-functionalized NHC ligand (Scheme 6) showed catalytic activities up to 260 (g of C₂H₄)/(g of Ni) after 1 h in ethylene

Scheme 6. Nonfunctionalized NHC Ligand Associated with Ni(II) in Catalytic Olefin Oligomerization



oligomerization, upon activation with MMAO in toluene.^{37d} Other systems turned out to be poorly active.^{37b} Furthermore, square-planar Ni(II) complexes with nonfunctionalized NHC ligands (Scheme 6) were revealed to be poorly active catalysts for 1-butene dimerization upon activation with AlEt_2Cl in toluene (after 30 min, maximum TON = 50 (mol of C_4H_{10})/(mol of Ni)).³⁹ The activity could be increased when the imidazolium-based ionic liquid was used as solvent (TON up to 3510 (mol of C_4H_{10})/(mol of Ni) after 30 min).³⁹ Styrene oligomerization was catalyzed by an allyl Ni–NHC complex with a TOF of 748 (mol of styrene)/(mol of Ni) h (Scheme 6).⁴⁰ Nonfunctionalized NHC–Ni complexes may also catalyze the polymerization of various alkenes.^{40,41}

Although the presence of lithium in complexes **10–12** could alter the electronic density at the alkoxy sites and, by extension, the catalytic activities observed in ethylene oligomerization, these complexes could unfortunately not be tested, owing to difficulties in obtaining suitable samples, in terms of quantity or purity.

CONCLUSION

We have prepared palladium(II) alcohol- or alcoholate-functionalized NHC complexes which display an excellent stability toward air and moisture. It was possible to selectively deprotonate and coordinate or reprotonate and decoordinate the alkoxide side chain using acid–base reactions, without affecting the Pd– C_{NHC} bond. The only Ni(II) complex isolated with an alcohol-functionalized NHC ligand was the square-planar complex $[\text{NiCl}_2\{\text{ImDiPP}(\text{C}_2\text{OH})\text{-C}_{\text{NHC}}\}_2]$ (**13**), in which only the C_{NHC} atom is bound to the metal. New nickel(II) alcoholate-functionalized NHC complexes have also been described, but their synthesis was rather challenging and only the dinuclear Ni(II) complex **8** could be obtained in good yield and fully characterized. Its catalytic performance for ethylene oligomerization showed, by comparison with literature data for nonfunctionalized NHCs, that the presence of a $\text{C}_{\text{NHC}}\text{O}$ chelate and/or alcoholate bridge led to improved properties. This may be due to the increased lifetime of the catalyst. However, it remains impossible to state the exact bonding situation in the active species. The carbene– Ni^{II} bond was found to be significantly less robust than the corresponding carbene– Pd^{II} bond. The mixed Ni(II)–Li(I) complexes **10–12** were also isolated, although in low yield, and characterized by X-ray diffraction. These Ni(II) complexes proved to be very sensitive in solution. Owing to the synthetic difficulties associated with the synthesis of nickel(II) alcohol- or alcoholate-functionalized NHC complexes, the replacement of this oxygen functionalization by an ether group is currently under investigation, and preliminary results show that such complexes are active catalysts in ethylene oligomerization.

ASSOCIATED CONTENT

Supporting Information

Text, figures, tables, and CIF files giving experimental details and NMR data for all compounds prepared in this paper and crystallographic data and ORTEP views of **2**· $2\text{H}_2\text{O}$, **3**, **4**, **4-polymorph**, **5**, **6**· CH_2Cl_2 , and **8–13**. This material is available free of charge via the Internet at <http://pubs.acs.org>. CIF files have also been deposited with the CCDC, 12 Union Road, Cambridge CB2 1EZ, U.K., and can be obtained on request free of charge, by quoting the publication citation and deposition numbers 975961–975972.

AUTHOR INFORMATION

Corresponding Author

*E-mail for P.B.: braunstein@unistra.fr.

Notes

The authors declare no competing financial interest.

ACKNOWLEDGMENTS

The Centre National de la Recherche Scientifique (CNRS), the Ministère de l'Enseignement Supérieur et de la Recherche (Ph.D. fellowship to S.H.), and IFP Energies nouvelles (IFPEN) are gratefully acknowledged for support. We thank Mélanie Boucher and Marc Mermillon-Fournier for experimental support. The NMR service of the Université de Strasbourg is warmly acknowledged for the 2D correlation experiments.

REFERENCES

- (1) (a) Pugh, D.; Danopoulos, A. A. *Coord. Chem. Rev.* **2007**, *251*, 610–641. (b) Liddle, S. T.; Edworthy, I. S.; Arnold, P. L. *Chem. Soc. Rev.* **2007**, *36*, 1732–1744. (c) Normand, A. T.; Cavell, K. J. *Eur. J. Inorg. Chem.* **2008**, 2781–2800. (d) Corberán, R.; Mas-Marzá, E.; Peris, E. *Eur. J. Inorg. Chem.* **2009**, 1700–1716. (e) John, A.; Ghosh, P. *Dalton Trans.* **2010**, 39, 7183–7206. (f) Bierenstiel, M.; Cross, E. D. *Coord. Chem. Rev.* **2011**, *255*, 574–590. (g) Fliedel, C.; Braunstein, P. *J. Organomet. Chem.* **2014**, *751*, 286–300.
- (2) (a) Douthwaite, R. E.; Green, M. L. H.; Silcock, P. J.; Gomes, P. T. *Dalton Trans.* **2002**, 1386–1390. (b) Crudden, C. M.; Allen, D. P. *Coord. Chem. Rev.* **2004**, *248*, 2247–2273.
- (3) (a) Braunstein, P.; Naud, F. *Angew. Chem., Int. Ed.* **2001**, *40*, 680–699. (b) Kühn, O. *Chem. Soc. Rev.* **2007**, *36*, 592–607.
- (4) (a) Chen, C.; Qiu, H.; Chen, W.; Wang, D. *J. Organomet. Chem.* **2008**, *693*, 3273–3280. (b) Zhang, C.; Wang, Z.-X. *Organometallics* **2009**, *28*, 6507–6514. (c) Li, F.; Hu, J. J.; Koh, L. L.; Hor, T. S. A. *Dalton Trans.* **2010**, 39, 5231–5241. (d) Chen, C.; Qiu, H.; Chen, W. *Inorg. Chem.* **2011**, *50*, 8671–8678. (e) Benítez Junquera, L.; Puerta, M. C.; Valerga, P. *Organometallics* **2012**, *31*, 2175–2183.
- (5) (a) Lee, C. C.; Ke, W. C.; Chan, K. T.; Lai, C. L.; Hu, C. H.; Lee, H. *Chem. Eur. J.* **2007**, *13*, 582–591. (b) Ahmida, A.; Withake, D.; Flörke, U.; Egold, H.; Henkel, G. *Acta Crystallogr., Sect. E* **2012**, *68*, m975.
- (6) (a) O, W. W. N.; Lough, A. J.; Morris, R. H. *Organometallics* **2009**, *28*, 6755–6761. (b) Huang, Y.-P.; Tsai, C.-C.; Shih, W.-C.; Chang, Y.-C.; Lin, S.-T.; Yap, G. P. A.; Chao, I.; Ong, T.-G. *Organometallics* **2009**, *28*, 4316–4323.
- (7) (a) Liao, C.-Y.; Chan, K.-T.; Chang, Y.-C.; Chen, C.-Y.; Tu, C.-Y.; Hu, C.-H.; Lee, H. M. *Organometallics* **2007**, *26*, 5826–5833. (b) Berding, J.; van Dijkman, T. F.; Lutz, M.; Spek, A. L.; Bouwman, E. *Dalton Trans.* **2009**, 6948–6955. (c) Ray, S.; Shaikh, M. M.; Ghosh, P. *Eur. J. Inorg. Chem.* **2009**, 1932–1941. (d) Kumar, S.; Narayanan, A.; Rao, M. N.; Shaikh, M. M.; Ghosh, P. *J. Organomet. Chem.* **2012**, *696*, 4159–4165.
- (8) Badaj, A. C.; Lavoie, G. G. *Organometallics* **2012**, *31*, 1103–1111.

- (9) (a) Ray, L.; Shaikh, M. M.; Ghosh, P. *Dalton Trans.* **2007**, 4546–4555. (b) Yang, W.-H.; Lee, C.-S.; Pal, S.; Chen, Y.-N.; Hwang, W.-S.; Lin, I. J. B.; Wang, J.-C. *J. Organomet. Chem.* **2008**, 693, 3729–3740. (c) Lee, J. H.; Yoo, K. S.; Park, C. P.; Olsen, J. M.; Sakaguchi, S.; Prakash, G. K. S.; Mathew, T.; Jung, K. W. *Adv. Synth. Catal.* **2009**, 351, 563–568.
- (10) (a) Schwarz, J.; Böhm, V. P. W.; Gardiner, M. G.; Grosche, M.; Herrmann, W. A.; Hieringer, W.; Raudaschl-Sieber, G. *Chem. Eur. J.* **2000**, 6, 1773–1780. (b) Glas, H.; Herdtweck, E.; Spiegler, M.; Pleier, A.-K.; Thiel, W. R. *J. Organomet. Chem.* **2001**, 626, 100–105. (c) Arnold, P. L.; Sanford, M. S.; Pearson, S. M. *J. Am. Chem. Soc.* **2009**, 131, 13912–13913. (d) Sakaguchi, S.; Kawakami, M.; O'Neill, J.; Yoo, K. S.; Jung, K. W. *J. Organomet. Chem.* **2010**, 695, 195–200. (e) Jokić, N. B.; Straubinger, C. S.; Li Min Goh, S.; Herdtweck, E.; Herrmann, W. A.; Kühn, F. E. *Inorg. Chim. Acta* **2010**, 363, 4181–4188. (f) Peñafiel, I.; Pastor, I. M.; Yus, M.; Esteruelas, M. A.; Oliván, M.; Oñate, E. *Eur. J. Org. Chem.* **2011**, 7174–7181.
- (11) Ketz, B. E.; Cole, A. P.; Waymouth, R. M. *Organometallics* **2004**, 23, 2835–2837.
- (12) Boydston, A. J.; Rice, J. D.; Sanderson, M. D.; Dykhno, O. L.; Bielawski, C. W. *Organometallics* **2006**, 25, 6087–6098.
- (13) (a) Waltman, A. W.; Grubbs, R. H. *Organometallics* **2004**, 23, 3105–3107. (b) Ren, H.; Yao, P.; Xu, S.; Song, H.; Wang, B. *J. Organomet. Chem.* **2007**, 692, 2092–2098. (c) Kong, Y.; Wen, L.; Song, H.; Xu, S.; Yang, M.; Liu, B.; Wang, B. *Organometallics* **2011**, 30, 153–159.
- (14) (a) Kantchev, E. A. B.; O'Brien, C. J.; Organ, M. G. *Angew. Chem., Int. Ed.* **2007**, 46, 2768–2813. (b) Marion, N.; Nolan, S. P. *Acc. Chem. Res.* **2008**, 41, 1440–1449.
- (15) Khlebnikov, V.; Meduri, A.; Mueller-Bunz, H.; Montini, T.; Fornasiero, P.; Zangrando, E.; Milani, B.; Albrecht, M. *Organometallics* **2012**, 31, 976–986.
- (16) (a) Skupinska, J. *Chem. Rev.* **1991**, 91, 613–648. (b) *Applied Homogeneous Catalysis with Organometallic Compounds*, 2nd ed.; Cornils, B., Hermann, W. A., Eds.; Wiley-VCH: Weinheim, Germany, 2002. (c) Vogt, D. In *Aqueous Phase Organometallic Catalysis-Concepts and Applications*, 2nd ed.; Cornils, B., Hermann, W. A., Eds.; Wiley-VCH: Weinheim, Germany, 2004. (d) Lappin, G. R.; Nemeč, L. H.; Sauer, J. D.; Wagner, J. D. Higher Olefins. In *Kirk-Othmer Encyclopedia of Chemical Technology*; Wiley: Hoboken, NJ, 2005. (e) Keim, W. *Angew. Chem., Int. Ed.* **2013**, 52, 12492–12496.
- (17) (a) Li, W.; Sun, H.; Chen, M.; Wang, Z.; Hu, D.; Shen, Q.; Zhang, Y. *Organometallics* **2005**, 24, 5925–5928. (b) Samantaray, M. K.; Shaikh, M. M.; Ghosh, P. *Organometallics* **2009**, 28, 2267–2275.
- (18) (a) Ketz, B. E.; Ottenwaelder, X. G.; Waymouth, R. M. *Chem. Commun.* **2005**, 5693–5695. (b) Benson, S.; Payne, B.; Waymouth, R. M. *J. Polym. Sci., Part A: Polym. Chem.* **2007**, 45, 3637–3647. (c) Shanmuganathan, S.; Köhl, O.; Jones, P. G.; Heinicke, J. *Cent. Eur. J. Chem.* **2010**, 8, 992–998.
- (19) (a) Li, W.-F.; Sun, H.-M.; Wang, Z.-G.; Chen, M.-Z.; Shen, Q.; Zhang, Y. *J. Organomet. Chem.* **2005**, 690, 6227–6232. (b) Zhang, D.; Kawaguchi, H. *Organometallics* **2006**, 25, 5506–5509. (c) Waltman, A. W.; Ritter, T.; Grubbs, R. H. *Organometallics* **2006**, 25, 4238–4239. (d) Boydston, A. J.; Rice, J. D.; Sanderson, M. D.; Dykhno, O. L.; Bielawski, C. W. *Organometallics* **2006**, 25, 6087–6098.
- (20) (a) Arnold, P. L.; Scarisbrick, A. C.; Blake, A. J.; Wilson, C. *Chem. Commun.* **2001**, 2340–2341. (b) Arnold, P. L.; Scarisbrick, A. C. *Organometallics* **2004**, 23, 2519–2521. (c) Arnold, P. L.; Blake, A. J.; Wilson, C. *Chem. Eur. J.* **2005**, 11, 6095–6099. (d) Jones, N. A.; Liddle, S. T.; Wilson, C.; Arnold, P. L. *Organometallics* **2007**, 26, 755–757. (e) Arnold, P. L.; Casely, I. J.; Turner, Z. R.; Bellabarba, R.; Tooze, R. B. *Dalton Trans.* **2009**, 7236–7247. (f) Arnold, P. L.; Casely, I. J.; Zlatogorsky, S.; Wilson, C. *Helv. Chim. Acta* **2009**, 92, 2291–2303. (g) Benítez, M.; Mas-Marzá, E.; Mata, J. A.; Peris, E. *Chem. Eur. J.* **2011**, 17, 10453–10461.
- (21) (a) Song, H.; Fan, D.; Liu, Y.; Hou, G.; Zi, G. *J. Organomet. Chem.* **2013**, 729, 40–45. (b) Arduengo, A. J.; Dolphin, J. S.; Gurău, G.; Marshall, W. J.; Nelson, J. C.; Petrov, V. A.; Runyon, J. W. *Angew. Chem., Int. Ed.* **2013**, 52, 5110–5114.
- (22) (a) Ittel, S. D.; Johnson, L. K.; Brookhart, M. *Chem. Rev.* **2000**, 100, 1169–1204. (b) Chen, E. Y.-X.; Marks, T. J. *Chem. Rev.* **2000**, 100, 1391–1434. (c) Speiser, F.; Braunstein, P.; Saussine, L. *Acc. Chem. Res.* **2005**, 38, 784–793. (d) Bianchini, C.; Giambastiani, G.; Rios, I. G.; Mantovani, G.; Meli, A.; Segarra, A. M. *Coord. Chem. Rev.* **2006**, 250, 1391–1418. (e) Bianchini, C.; Giambastiani, G.; Luconi, L.; Meli, A. *Coord. Chem. Rev.* **2010**, 254, 431–455. (f) Wang, S.; Sun, W.-H.; Redshaw, C. *J. Organomet. Chem.* **2014**, 751, 717–741.
- (23) (a) Marion, N.; Ecarnot, E. C.; Navarro, O.; Amoroso, D.; Bell, A.; Nolan, S. P. *J. Org. Chem.* **2006**, 71, 3816–3821. (b) Marion, N.; de Frémont, P.; Puijk, I. M.; Ecarnot, E. C.; Amoroso, D.; Bell, A.; Nolan, S. P. *Adv. Synth. Catal.* **2007**, 349, 2380–2384.
- (24) (a) Arnold, P. L.; Rodden, M.; Davis, K. M.; Scarisbrick, A. C.; Blake, A. J.; Wilson, C. *Chem. Commun.* **2004**, 1612–1613. (b) Zhao, D.; Fei, Z.; Scopelliti, R.; Dyson, P. J. *Inorg. Chem.* **2004**, 43, 2197–2205. (c) Ray, L.; Katiyar, V.; Raihan, M. J.; Nanavati, H.; Shaikh, M. M.; Ghosh, P. *Eur. J. Inorg. Chem.* **2006**, 3724–3730.
- (25) Navarro, O.; Marion, N.; Scott, N. M.; Gonzalez, J.; Amoroso, D.; Bell, A.; Nolan, S. P. *Tetrahedron* **2005**, 61, 9716–9722.
- (26) (a) Sakaguchi, S.; Yoo, K. S.; O'Neill, J.; Lee, J. H.; Stewart, T.; Jung, K. W. *Angew. Chem., Int. Ed.* **2008**, 47, 9326–9329. (b) Yoo, K. S.; O'Neill, J.; Sakaguchi, S.; Giles, R.; Lee, J. H.; Jung, K. W. *J. Org. Chem.* **2009**, 75, 95–101. (c) de K. Lewis, A. K.; Caddick, S.; Esposito, O.; Cloke, F. G. N.; Hitchcock, P. B. *Dalton Trans.* **2009**, 7094–7098.
- (27) (a) Bettucci, L.; Bianchini, C.; Oberhauser, W.; Hsiao, T.-H.; Lee, H. M. *J. Mol. Catal. A: Chem.* **2010**, 322, 63–72. (b) Egbert, J. D.; Chartoire, A.; Slawin, A. M. Z.; Nolan, S. P. *Organometallics* **2011**, 30, 4494–4496. (c) Cross, W. B.; Daly, C. G.; Ackerman, R. L.; George, I. R.; Singh, K. *Dalton Trans.* **2011**, 40, 495–505.
- (28) (a) Li, D.; Liu, D. *J. Chem. Crystallogr.* **2003**, 33, 989–991. (b) Tulloch, A. A. D.; Winston, S.; Danopoulos, A. A.; Eastham, G.; Hursthouse, M. B. *Dalton Trans.* **2003**, 699–708. (c) Yang, X.; Fei, Z.; Geldbach, T. J.; Phillips, A. D.; Hartinger, C. G.; Li, Y.; Dyson, P. J. *Organometallics* **2008**, 27, 3971–3977. (d) Fliedel, C.; Schnee, G.; Braunstein, P. *Dalton Trans.* **2009**, 2474–2476. (e) Samantaray, M. K.; Shaikh, M. M.; Ghosh, P. *J. Organomet. Chem.* **2009**, 694, 3477–3486. (f) Szulmanowicz, M. S.; Gniewek, A.; Gil, W.; Trzeciak, A. M. *ChemCatChem* **2013**, 5, 1152–1160.
- (29) (a) McGuinness, D. S.; Green, M. J.; Cavell, K. J.; Skelton, B. W.; White, A. H. *J. Organomet. Chem.* **1998**, 565, 165–178. (b) Altenhoff, G.; Goddard, R.; Lehmann, C. W.; Glorius, F. *J. Am. Chem. Soc.* **2004**, 126, 15195–15201. (c) Yang, W.-H.; Lee, C.-S.; Pal, S.; Chen, Y.-N.; Hwang, W.-S.; Lin, I. J. B.; Wang, J.-C. *J. Organomet. Chem.* **2008**, 693, 3729–3740.
- (30) (a) Houghton, J.; Dyson, G.; Douthwaite, R. E.; Whitwood, A. C.; Kariuki, B. M. *Dalton Trans.* **2007**, 3065–3073. (b) Huynh, H. V.; Yuan, D.; Han, Y. *Dalton Trans.* **2009**, 7262–7268. (c) Warsink, S.; de Boer, S. Y.; Jongens, L. M.; Fu, C.-F.; Liu, S.-T.; Chen, J.-T.; Lutz, M.; Spek, A. L.; Elsevier, C. J. *Dalton Trans.* **2009**, 7080–7086. (d) Yuan, D.; Huynh, H. V. *Organometallics* **2010**, 29, 6020–6027. (e) Yuan, D.; Tang, H.; Xiao, L.; Huynh, H. V. *Dalton Trans.* **2011**, 40, 8788–8795. (f) Yuan, D.; Huynh, H. V. *Dalton Trans.* **2011**, 40, 11698–11703.
- (31) Hameury, S.; de Frémont, P.; Breuil, P.-A. R.; Olivier-Bourbigou, H.; Braunstein, P. *Dalton Trans.* **2014**, 43, 4700–4710.
- (32) Arnold, P. L.; Rodden, M.; Davis, K. M.; Scarisbrick, A. C.; Blake, A. J.; Wilson, C. *Chem. Commun.* **2004**, 1612–1613.
- (33) Yuan, D.; Huynh, H. V. *Inorg. Chem.* **2013**, 52, 6627–6634.
- (34) Henrion, M.; Oertel, A. M.; Ritleng, V.; Chetcuti, M. J. *Chem. Commun.* **2013**, 49, 6424–6426.
- (35) (a) Jubb, J.; Gambarotta, S. *Inorg. Chem.* **1994**, 33, 2503–2504. (b) Blake, A. J.; Mountford, P.; Nikonov, G. I. *Acta Crystallogr., Sect. C* **1996**, C52, 1911–1913. (c) Aspinall, H. C.; Bickley, J. F.; Gaskell, J. M.; Jones, A. C.; Labat, G.; Chalker, P. R.; Williams, P. A. *Inorg. Chem.* **2007**, 46, 5852–5860.
- (36) (a) Herrmann, W. A.; Gerstberger, G.; Spiegler, M. *Organometallics* **1997**, 16, 2209–2212. (b) Matsubara, K.; Ueno, K.; Shibata, Y. *Organometallics* **2006**, 25, 3422–3427.
- (37) (a) McGuinness, D. S.; Mueller, W.; Wasserscheid, P.; Cavell, K. J.; Skelton, B. W.; White, A. H.; Englert, U. *Organometallics* **2002**, 21,

175–181. (b) MacKinnon, A. L.; Baird, M. C. *J. Organomet. Chem.* **2003**, 683, 114–119. (c) Cavell, K. J.; McGuinness, D. S. *Coord. Chem. Rev.* **2004**, 248, 671–681. (d) Sun, H. M.; Shao, Q.; Hu, D. M.; Li, W. F.; Shen, Q.; Zhang, Y. *Organometallics* **2005**, 24, 331–334. (e) Li, W.-F.; Sun, H.-M.; Chen, M.-Z.; Shen, Q.; Zhang, Y. *J. Organomet. Chem.* **2008**, 693, 2047–2051.

(38) Miyake, G. M.; Akhtar, M. N.; Fazal, A.; Jaseer, E. A.; Daeffler, C. S.; Grubbs, R. H. *J. Organomet. Chem.* **2013**, 728, 1–5.

(39) McGuinness, D. S.; Mueller, W.; Wasserscheid, P.; Cavell, K. J.; Skelton, B. W.; White, A. H.; Englert, U. *Organometallics* **2002**, 21, 175–181.

(40) Càmpora, J.; Ortiz de la Tabla, L.; Palma, P.; Alvarez, E.; Lahoz, F.; Mereiter, K. *Organometallics* **2006**, 25, 3314–3316.

(41) (a) Buchowicz, W.; Koziol, A.; Jerzykiewicz, L. B.; Lis, T.; Pasynkiewicz, S.; Pęcherzewska, A.; Pietrzykowski, A. *J. Mol. Catal. A: Chem.* **2006**, 257, 118–123. (b) Sujith, S.; Noh, E. K.; Lee, B. Y.; Han, J. W. *J. Organomet. Chem.* **2008**, 693, 2171–2176. (c) Buchowicz, W.; Wojtczak, W.; Pietrzykowski, A.; Lupa, A.; Jerzykiewicz, L. B.; Makal, A.; Wozniak, K. *Eur. J. Inorg. Chem.* **2010**, 648–656. (d) Berding, J.; Lutz, M.; Spek, A. L.; Bouwman, E. *Appl. Organomet. Chem.* **2011**, 25, 76–81. (e) Zhang, D.; Zhou, S.; Li, Z.; Wang, Q.; Weng, L. *Dalton Trans.* **2013**, 42, 12020–12030. (f) Buchowicz, W.; Conder, J.; Hryciuk, D.; Zachara, J. *J. Mol. Catal. A: Chem.* **2014**, 381, 16–20.

■ NOTE ADDED AFTER ASAP PUBLICATION

This paper was published on the Web April 25, 2014, with minor text errors. The corrected version was reposted on April 28, 2014.